Supplementary data

ROOOH: the Missing Piece of the Puzzle for OH measurements in low NO Environments

Christa Fittschen[1], Mohamad Al Ajami[1], Sebastien Batut[1], Valerio Ferracci[2,3], Scott Archer-Nicholls[2], Alexander T. Archibald[2,4], Coralie Schoemaecker[1]

[1]Université Lille, CNRS, UMR 8522 - PC2A - Physicochimie des Processus de Combustion et de l'Atmosphère, F-59000 Lille, France
[2] University of Cambridge, Centre for Atmospheric Science, Department of Chemistry, Lensfield Road, Cambridge, CB2 1EW, UK
[3] Cranfield University, Centre for Environmental and Agricultural Informatics, College Road, Cranfield MK43 0AL, UK
[4] National Centre for Atmospheric Science, Cambridge, UK

*Corresponding author: Christa Fittschen (christa.fittschen@univ-lille1.fr)
Tel: ++ 33 3 20 33 72 66

1.) FAGE pump and probe system

Details of the ULille FAGE pump and probe system have been described in detail elsewhere publications (Fuchs et al., 2017;Hansen et al., 2015;Parker et al., 2011)

Briefly, the FAGE instrument is coupled to a photolysis cell (**Figure S1**), in which a plume of OH is generated by 266 nm photolysis of ozone in presence of water vapor. Time-resolved OH decays are monitored at a temporal resolution of 200 µs using the high repetition rate probe laser (5 kHz) of the FAGE instrument. The photolysis cell is a 50-cm long, 5 cm-i.d. cylindrical tube made of aluminum. A Suprasil quartz window is mounted on one side of the cell, and the other side is directly connected to the FAGE nozzle. The pressure in the photolysis cell is around 745 Torr, and pumping from the FAGE instrument (3 L min^{-1}), the O_3 analyzer (0.3 L min^{-1}) and the hygrometer (0.4 L min^{-1}) ensures that the photolysis cell is continuously flushed with gas mixture. The residence time within the photolysis cell is around 20 sec, *i.e*. at a photolysis repetition rate of 2 Hz, the gas mixture is photolysed around 40 times before it enters the FAGE detection cell. Experiments have been carried out by first covering the photolysis laser in order to start each series with a fresh mixture.

OH is generated inside the cell by ozone photolysis at 266 nm in the presence of water vapor (reactions (RS1) and (RS2)) using a quadrupled YAG laser (Quantel, YG 981C) operated at a pulse repetition rate of 2 Hz.

$$O_3 + h\nu_{266nm} \rightarrow O_2 + O(^1D) \qquad \text{(RS1)}$$

$$O(^1D) + H_2O \rightarrow 2\ OH \qquad \text{(RS2)}$$

An ozone mixing ratio of at least 600 ppbv is maintained inside the photolysis cell by injecting a small flow rate of 20 mL min^{-1} (negligible compared to the main flow through the reactor) of concentrated ozone using an ozone generator (Scientech). A water vapor mixing ratio of about 12000 ppmv is injected in the cell by passing a part of the air through a bubbler. The energy of the photolysis laser was set to 20 mJ $pulse^{-1}$ for a beam diameter of 2.5 cm, which was achieved after expansion through a telescope. This expansion of the beam allows the generation of OH in a cylindrical volume that is larger than the FAGE nozzle (0.4 mm) in order to probe a more homogeneous volume with respect to the OH concentration, even if the shape of the beam involves a Gaussian distribution. The pulse duration of the photolysis laser is 20 ns (full-width half maximum).

The photolysis cell is coupled with an airtight connection to the FAGE nozzle where OH is measured by LIF (Laser Induced Fluorescence) using the $Q_1(3)$ transition ($A^2\Sigma_+(v=0)–X^2\Pi(v=0)$) at 308 nm after gas expansion into a low pressure cell (0.3 mbar). The laser light is generated using a frequency-doubled dye laser (Sirah Laser PrecisionScan PRSC-24- HPR) pumped by the frequency-doubled output of a Nd:YVO_4 laser (Spectra Physics Navigator II YHP40- 532QW). The laser power used to probe OH was approximately 2 mW.

Hydrocarbons are added to the photolysis cell through calibrated flow meter, either directly from the gas cylinder (CH_4 and n-C_4H_{10} for a series of experiments) or from a canister in which a diluted gas mixture of n-C_4H_{10} or isoprene had been prepared manometrically.

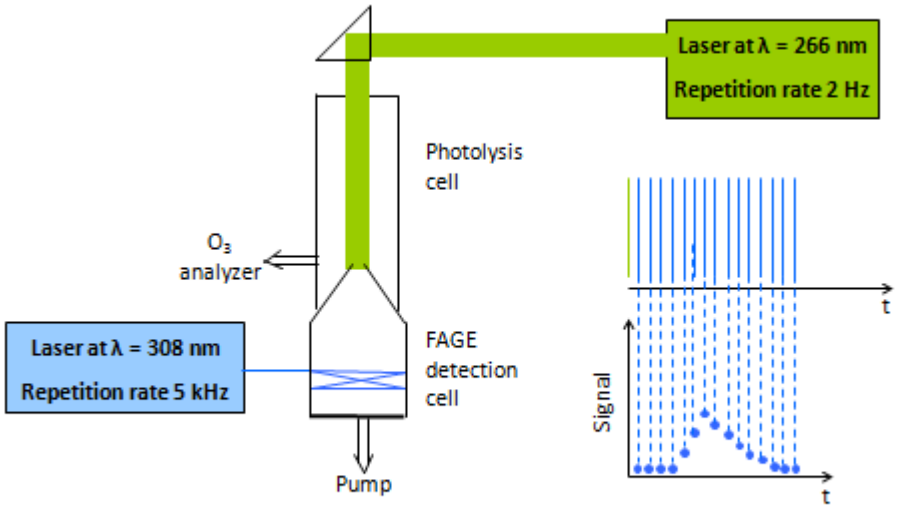

Figure S1: Schematic view of the ULille FAGE pump and probe instrument

2.) LIF Calibration procedure

In order to access the absolute concentrations of OH radicals, calibrations are made using a calibration cell in which air of known water vapour concentration is photolysed at 184.9 nm by a mercury lamp, producing an equal and known concentration of OH and HO_2. The lamp flux is indirectly measured by actinometry on ozone, produced simultaneously by oxygen photolysis at the same wavelength. For calibration purposes, the photolysis cell is unmounted and the calibration cell is placed in front of the FAGE nozzle. Very high flow of synthetic air (40 l min^{-1}) is flowed through the calibration cell to assure (a) turbulent flow conditions within the calibration cell and (b) that the entire gas intake by the FAGE consists of calibration gas. Details on FAGE calibration procedure can be found elsewhere *(Dusanter et al., 2008)*.

3.) Complementary experiments with Isoprene:

a: Measurements under different conditions: is the interference a 1- or 2-photon process?

In order to check whether the observed increase in background fluorescence is a 1- or 2-photon process, i.e. due to interference by photolysis or by decomposition of an unknown species, we have carried out experiments with isoprene at the same condition (concentration and photolysis energy) but varying the fluorescence excitation laser energy and/or the repetition rate of the excitation laser.

In order to characterize the refreshing time in our FAGE instrument and to determine if photolytic interferences can be clearly identified, we have used acetone, CH_3COCH_3, known to lead to photolytic

interference in the FAGE cell *(17)*, in separate experiments as tracer for OH radicals generated photolytically by the excitation laser within the FAGE cell. Acetone is photolysed at the excitation laser wavelength (308 nm):

$$CH_3COCH_3 \rightarrow CH_3CO + CH_3$$

with CH_3CO leading in subsequent reaction with O_2 to fast formation of OH with a yield close to 1 at zero pressure (Carr et al., 2007):

$$CH_3CO + O_2 \rightarrow \text{product} + OH$$

If the gas mixture in the excitation volume is not completely renewed between two shots (200µs), the OH radicals formed this way can be excited with one of the next excitation laser pulse. The resulting fluorescence intensity should (a) not be linear with the excitation laser fluence and (b) should decrease with decreasing repetition rate. This has been tested in our system with acetone:

a.) Clean air containing stable concentration of CH_3COCH_3 is pumped into the FAGE cell, and the resulting fluorescence intensity is plotted as a function of the laser power. **Figure S2** clearly shows a non-linear increase in fluorescence signal with laser power.

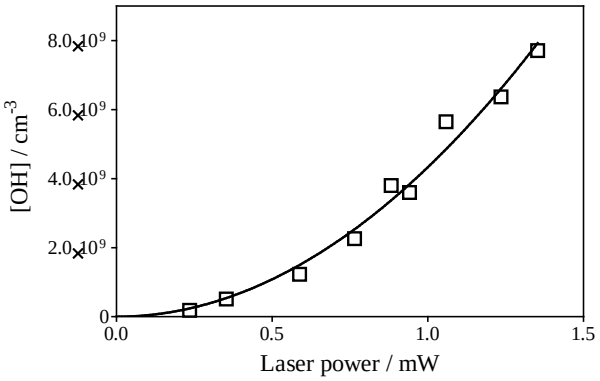

Figure S2: Formation of OH radicals from 308 nm photolysis of CH_3COCH_3 within the FAGE detection volume as a function laser energy within the FAGE cell. Repetition rate of the dye laser was 5 kHz, $[CH_3COCH_3] = 1.5\times10^{16}$ cm^{-3}.

b.) Clean air containing stable concentration of CH_3COCH_3 is pumped into the FAGE cell, and the resulting fluorescence is measured at different excitation laser repetition rates. In these experiments, the pump laser energy has been adapted to obtain the same pulse energy for different repetition rates. It can be seen that the OH concentration decreases, but even at 1 kHz, i.e. 1 ms between two excitation laser pulses, there is still a small OH signal is observed, as shown in **Figure S3**.

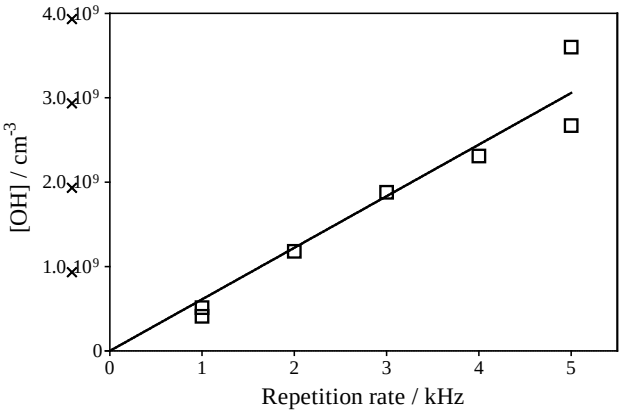

Figure S3: Formation of OH radicals from 308nm photolysis of CH_3COCH_3 as a function of the repetition rate. The YAG-laser energy has been adjusted in order to obtain for all repetition rates the same energy (0.8 mW within the FAGE cell). $[CH_3COCH_3] = 1.3\times10^{16}$ cm^{-3}.

From these experiments, it can be deduced that in the ULille FAGE photolytically generated OH radicals can be identified by either varying the fluence or the repetition rate of the fluorescence excitation laser.

In order to identify if similar interferences could explain the results of the experiments with isoprene, the same type of experiments have then been carried out with isoprene (3.2×10^{11} cm^{-3}) using two different laser energies at 5 kHz (1.7 and 0.8 mW) and with lower repetition rate (1 kHz, 0.4 mW). The results are shown in **Figure S4**.

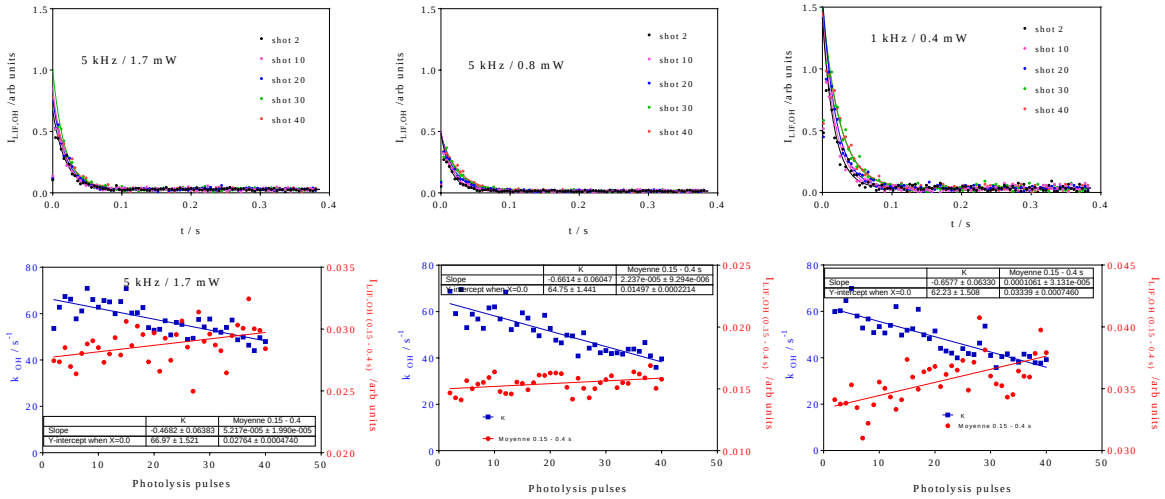

Figure S4: Photolysis of O_3 in the presence of isoprene using different excitation laser energies and repetition rates. Upper graphs: OH decays (for clarity, only every 10^{th} decay is shown), lower graph OH decay rate as a function of Photolysis pulses (blue dots, left y-axis) and fluorescence intensity averaged over 0.15 to 0.4 s (red dots, right y-axis).

The lower graphs shows the decrease in the decay rate with increasing number of photolysis pulses (blue dots), on the same order of magnitude for all three series, as expected (photolysis energies as well as isoprene and O_3 concentration were identical for all three series). Also, the background signal increases with increasing photolysis shots for all three series, but the slope is different. However, the

slope is directly proportional to the sensitivity of the LIF detection, and for comparison needs to be normalized to the initial OH intensity. The results are summarized in **Table S1**:

Table S1: Summary of results from **Figure S4**

Experiment	OH_0 LIF intensity [a]	Slope [b]	Slope / OH_0
5 kHz, 1.7 mW	0.85 ± 0.08	$(5.2\pm2.0) \times 10^{-5}$	$(6.1 \pm 2.5) \times 10^{-5}$
5 kHz, 0.8 mW	0.48 ± 0.04	$(2.2\pm0.9) \times 10^{-5}$	$(4.6 \pm 2.3) \times 10^{-5}$
1 kHz, 0.4 mW	1.50 ± 0.17	$(10.0\pm3.1) \times 10^{-5}$	$(6.7 \pm 2.7) \times 10^{-5}$

[a] OH_0 LIF intensity obtained as the average of the LIF intensity at t=0 for all 40 photolysis pulses, obtained by fitting to a single exponential decay between 0.01 – 0.4 s, in arbitrary units

[b]. Slope obtained by linear regression of red dots in **Figure S4**, in arbitrary units

From the observation that the increase in residual LIF signal with increasing number of photolysis pulses is independent of both (a) the fluorescence laser excitation energy and (b) the repetition rate of the excitation laser, we conclude that the observed interference is not due to a photolytic process.

b: Is the interference really due to the product of RO_2 + OH?

Experiments have been carried out with identical OH concentrations, but much higher isoprene concentration than in the above experiments. Under these conditions, there is still formation of high concentrations of RO_2, but as the isoprene concentration stays high, the RO_2 concentration never gets high enough to compete with the reaction of isoprene with OH. Therefore, one can expect formation of all products from RO_2 self- or cross reaction or reaction with HO_2, but only very little or no products from the reaction of RO_2 with OH.

The results are shown in **Figure S5**. For the conditions in the left graph ($[C_5H_8] = 1.23 \times 10^{12}$ cm^{-3}) the OH decay rate decreases ((-0.5±0.2) s^{-1} $pulse^{-1}$ = 20 s^{-1} after 40 pulses) in the same way than for the experiments above, and this is explained by the replacement of the reactive isoprene by less reactive products. For the conditions in the right graph the C_5H_8 concentration was so high ($[C_5H_8] = 1.23 \times 10^{13}$ cm^{-3}) that it leads to decay rates that are not measurable anymore with our time resolution. For both conditions however, the LIF-intensity at long times does not increase with the number of laser pulses ($(1.2\pm1.4) \times 10^{-5}$ and $(-1.3\pm1.2) \times 10^{-5}$ for the left and right graph, respectively).

From these observations, it can be concluded that the increase in LIF intensity at long reaction times is indeed due to the product of the reaction between RO_2 radicals and OH radicals.

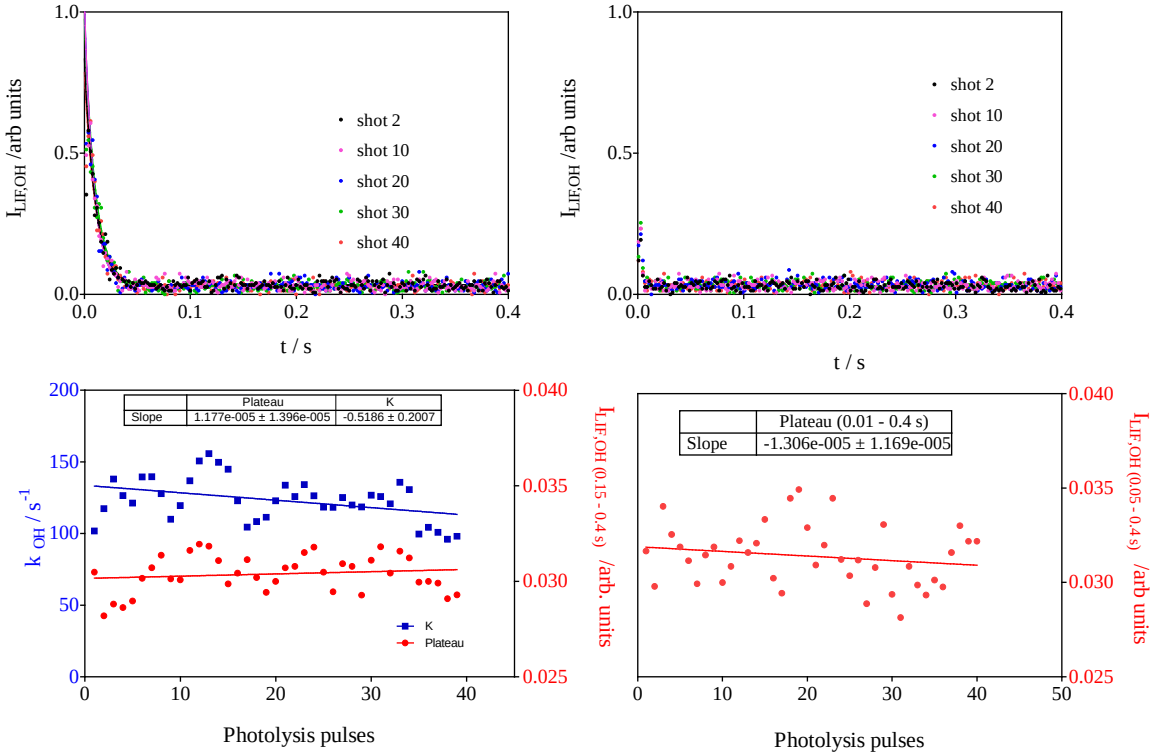

Figure S5: Experiments with high isoprene concentrations: $[C_5H_8]$ = 1.23 × $10^{12}$and 1.23 × 10^{13}molecule.cm^{-3} for left and right graph, respectively. Upper graph LIF signals as a function of the number of photolysis pulses (for clarity, only every 10^{th} pulse is shown), lower graph shows the rate constant in blue (left graph only, decay was too fast to be measurable under the conditions of the right graph) and the LIF intensity at long times (plateau from fitting for left graph, average of all data points between 0.01 – 0.4 s for right graph).

4. Modeling the chemistry in the photolysis cell

A very simple model was run to get a rough estimate of the concentration of ROOOH being produced within the photolysis cell under the conditions shown in **Figure 1** of the manuscript. The model assumes a yield of 1 for the formation of ROOOH by OH+RO_2 and a rate constant for OH+ROOOH estimated equivalent to the one of OH+CH_3OOH:

Table S2: Model used to estimate the accumulation of ROOOH in the photolysis cell before entering the FAGE cell, all rate constants have been taken from the most recent IUPAC evaluations (Atkinson et al., 2006;Atkinson et al., 2004)

Reaction	k / cm^3 s^{-1}
OH + Isoprene → RO_2	1 × 10^{-10}
OH + RO_2 → ROOOH	1 × 10^{-10}
OH + ROOOH → products	1 × $10^{-11, a}$
OH + O_3 → HO_2 + O_2	7.3 × 10^{-14}

$OH + HO_2 \rightarrow H_2O + O_2$	1×10^{-10}
$RO_2 + RO_2 \rightarrow$ products	1×10^{-12}
$RO_2 + HO_2 \rightarrow$ ROOH	1.7×10^{-11}

[a.] estimated equivalent to the rate constant of $OH+CH_3OOH$ *(S2)*

This model was run 40 times for 0.5 s, with the final concentrations of the different species obtained at each run being used as initial concentrations in the following run, always adding 1.4×10^{10} cm^{-3} OH radicals to the mixture and the evolution of the different species is shown in **Figure S6**.

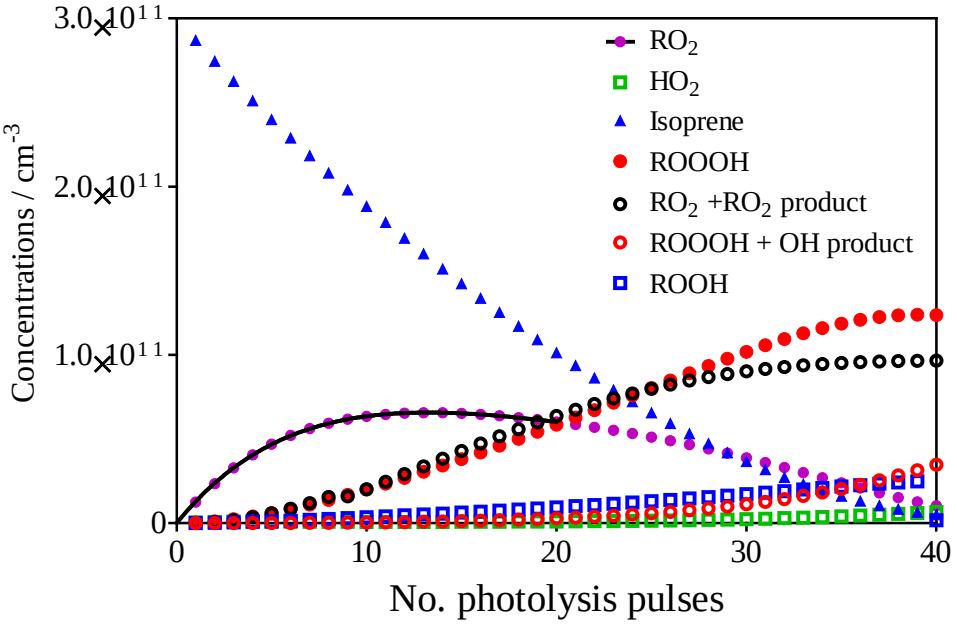

Figure S6: Evolution of different species in the photolysis cell as a function of the number of photolysis pulses. Full black line describes evolution of RO_2 by exponential rise (see section on CH_4 experiments)

The goal of this model is to get a good idea of how much ROOOH is possibly accumulated. The model has been run very basically: all OH radicals react with species present in the model, i.e. no wall loss or reaction with impurities is taken into account. The possible photolysis of ROOOH at 266 nm or a heterogeneous loss on the reactor walls is not taken into account. Also, no reaction of the products of RO_2 self reaction with OH are considered. Also, the possible inhomogeneity of the beam profile of our photolysis laser has not been considered, which can lead to uncertainties. All these simplifications can lead to an overestimation of the final ROOOH concentration, possibly up to a factor of 10. With these assumptions the model predicts the consumption of most isoprene, in line with the observed decrease of the OH decay rate of around 20 s^{-1} (**Figure 1** of the manuscript). The model predicts the formation of around [ROOOH] ≈ 1×10^{11} cm^{-3}. The other major reaction path for the RO_2 radicals under these conditions is the self-reaction. The reaction of ROOOH with OH radicals has been estimated (in comparison with ROOH) to 1×10^{-11} cm^3s^{-1}, but only a small fraction of ROOOH will have reacted with OH after 40 photolysis pulses.

5. Test with n-butane

The chemistry of RO_2 radicals with OH radicals is not very well investigated. For isoprene, the reaction products are not known at all, and the assumption made in this work that a trioxide is formed which subsequently leads to interference in the FAGE, is speculation based on a recent theoretical study. Assaf et al. (Assaf et al., 2018) highlighted an increase in stabilization of the adduct ROOOH formed by the reaction RO_2+OH with increasing size of the alkyl group between C_1 and C_4. This result is consistent with the measured HO_2 yield which decreased with increasing size of the alkyl moiety in the peroxy radical (C1 to C4). For butylperoxy radicals, the HO_2 yield was close to zero, leading to a supposed yield of ROOOH close to one. In the case of isoprene however one can still imagine the addition of OH radicals to the second double bond instead of reaction to the peroxy site and thus the yield of ROOOH may be less than one.

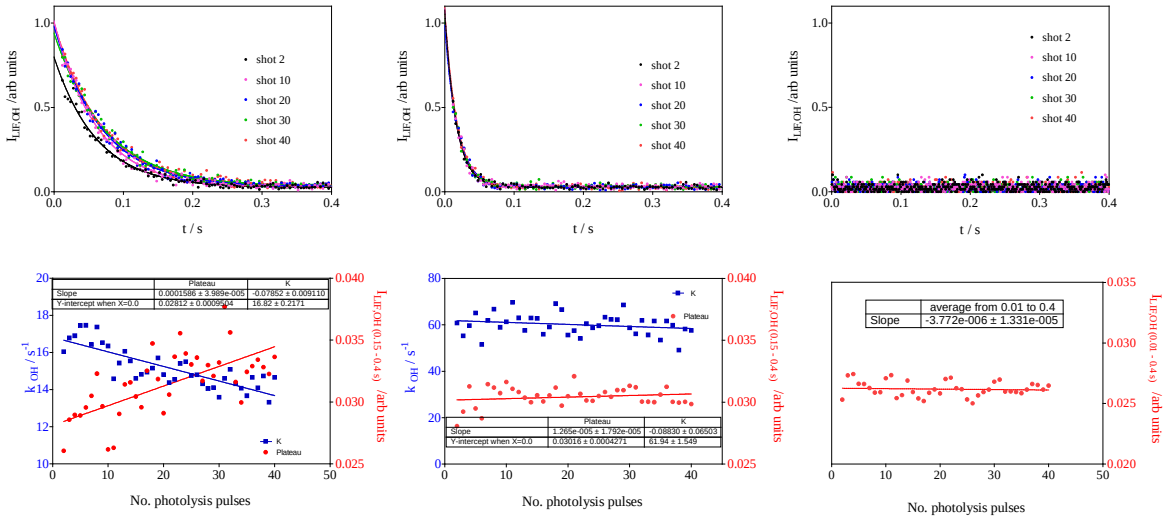

Figure S7: Photolysis of O_3 in the presence different concentrations of n-butane (7×10^{12}, $2 \times 10^{13}$and 7.5×10^{15} cm^{-3} from left to right). Upper graph: OH decays (for clarity only every 10^{th} decay is shown), lower graph: decay rates of OH radicals as a function of photolysis pulses (blue dots, left y-axis), residual LIF intensity taken from mono exponential fit for left graph and as the average LIF intensity between 0.15 – 0.4 s and 0.01 and 0.4 s for the center and right graph, respectively.

Therefore, we have investigated in the frame of this work the reaction of butane peroxy radicals with OH radicals. Different concentrations of butane have been added such that at the lowest concentration (left graphs in **Figure S7**) a high formation of ROOOH can be expected: under these conditions OH radicals react slowly with butane and the reaction with the nascent RO_2 radicals becomes rapidly competitive. The concentration has been increased in the middle graph of **Figure S7** such that only a low concentration of ROOOH is expected. In the right graph, finally, a very high concentration of butane has been used, too high to detect the decay of OH radicals with our time resolution. Under these conditions, it is expected that OH radicals react nearly exclusively with butane and no ROOOH is formed. Note that in all three experiments the initial OH radical concentration is the same. The interference is clearly visible in the left graph (slope m = (15.8±4)×10^{-5} arb. units), barely in the center graph (m = (1.2±1.7)×10^{-5} arb. units) and not present anymore in the right graph (m = -(0.4±1.3)×10^{-5} arb. units). Note that in the experiment of the right graph, the concentrations of all other species are similar to the concentrations in the left graph, i.e. the RO_2 and HO_2 concentrations are similar and with this all products obtained from self-and cross reactions. This

is a strong indicator that the observed increase in residual LIF intensity is indeed due to the product of the reaction of RO_2 with OH.

6. Test with CH_4

The reaction of CH_3O_2 + OH has been investigated in some detail (Assaf et al., 2017;Assaf et al., 2016) and it is now accepted that this reaction leads to formation of CH_3O + HO_2 (80-90%) with possibly small yield of CH_3OH and CH_3OOOH. Therefore, it is not expected to observe interference in the FAGE system. Two series of experiments with different CH_4 concentrations have been performed, the results are shown in **Figure S8**. In both series, one observes for the OH decay rate an increase over the first few photolysis shots. This is expected due to the formation of CH_3O_2 radicals that are more reactive than CH_4. In **Figure S6,** it can be seen that the model predicts (for an overall reactivity of 30 s^{-1}) an increase of RO_2 radicals over the first 10 pulses, followed by a steady state period and a slow decay. The decay rates are plotted as a function of the photolysis pulses in **Figure S8** (lower graphs) and have been fitted by forcing to the same rise time as the one obtained from the mono exponential fit of the RO_2 profile in **Figure S6**.A rough estimation of the increase in the decay rate of 8 s^{-1} is obtained, corresponding to a CH_3O_2 concentration (using $k(CH_3O_2+OH) = 1.5\times10^{-10}$ cm^3s^{-1}) (Assaf et al., 2016) of 5×10^{10} cm^{-3}, in excellent agreement with the predictions of the model, **Figure S6**. This good agreement gives more confidence in the principle idea of the experiments and the conditions chosen to enhance the formation of ROOOH.

In both series, the LIF intensity at long times does not change ($(-3.0\pm2.5\times10^{-5}$ and $1.0\pm1.7\times10^{-5}$ for left and right graph, respectively). This is expected due to the small yield of CH_3OOOH.

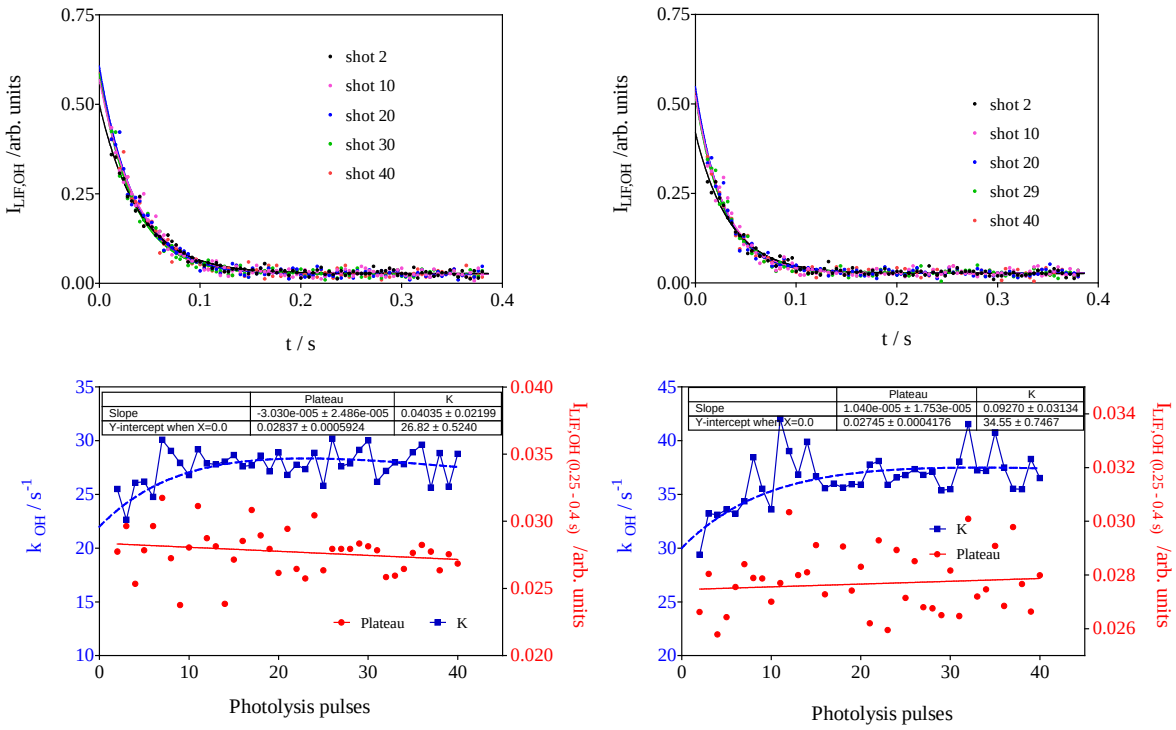

Figure S8: Photolysis of O_3 in the presence different concentrations of CH_4 (3.3×10^{15} cm^{-3} and 4.9×10^{15} cm^{-3} for the left and right graph, respectively). Upper graph: OH decays (for clarity only every 10^{th} decay is shown), lower graph: decay rates of OH radicals as a function of photolysis pulses (blue dots, left y-axis), residual LIF intensity taken as the average LIF intensity between 0.25 – 0.4s.

7. Global model simulations with varying ROOOH loss rates

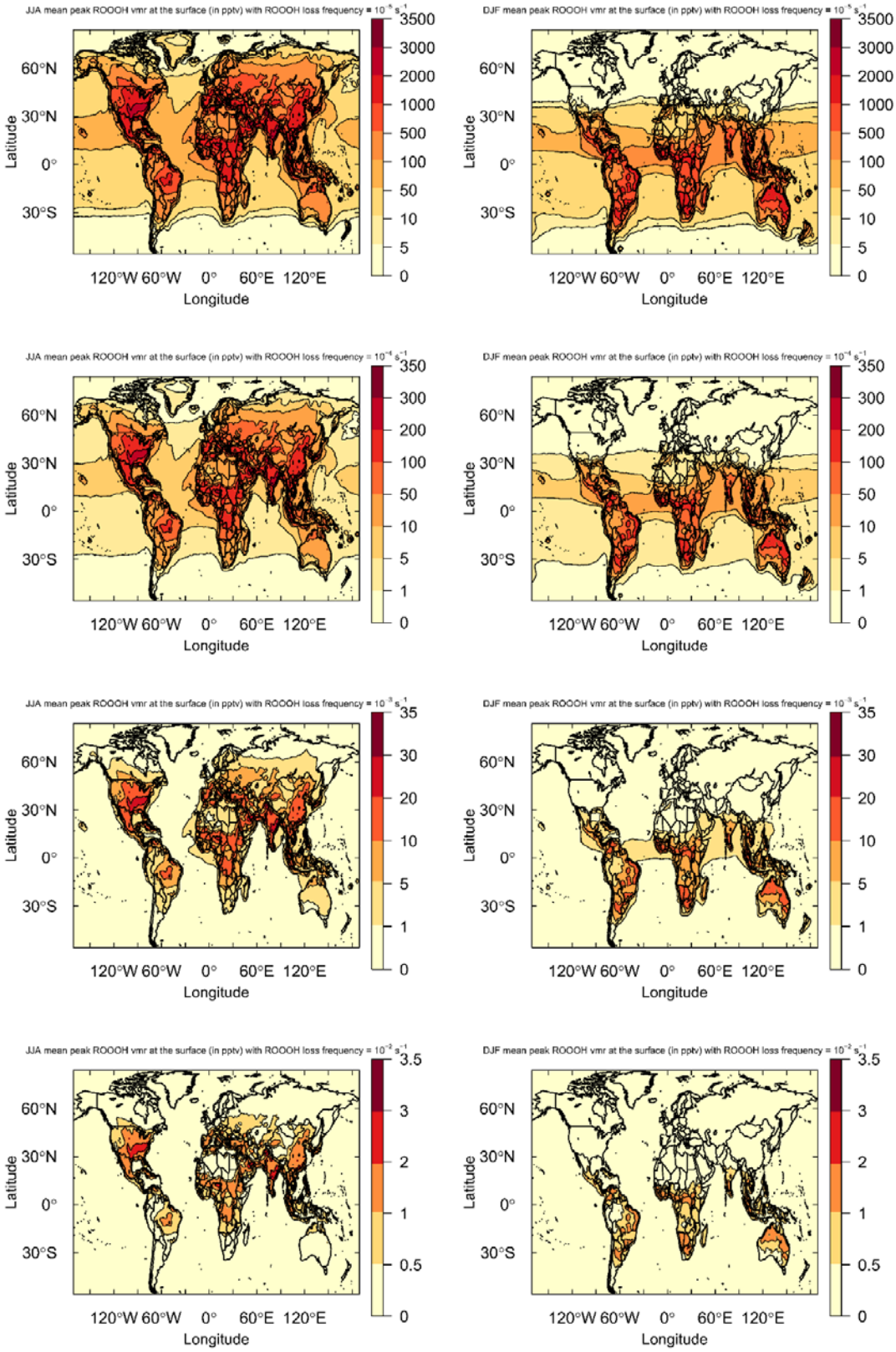

Figure S9: Modelled mean diurnal peak ROOOH volume mixing ratio (in ppt) during the Northern (left hand side) and Southern (right hand side) summer months. Each row shows steady state ROOOH abundances obtained with different ROOOH removal rates, ranging from 10^{-5} to 10^{-2} s^{-1}.

References

Assaf, E., Song, B., Tomas, A., Schoemaecker, C., and Fittschen, C.: Rate Constant of the Reaction between CH_3O_2 Radicals and OH Radicals revisited, J. Phys. Chem. A, 120, 8923-8932, 10.1021/acs.jpca.6b07704, 2016.

Assaf, E., Sheps, L., Whalley, L., Heard, D., Tomas, A., Schoemaecker, C., and Fittschen, C.: The Reaction between CH_3O_2 and OH Radicals: Product Yields and Atmospheric Implications, Environ. Sci. Technol., 51, 2170-2177, 10.1021/acs.est.6b06265, 2017.

Assaf, E., Schoemaecker, C., Vereecken, L., and Fittschen, C.: Experimental and Theoretical Investigation of the Reaction of RO_2 Radicals with OH Radicals: Dependence of the HO_2 Yield on the Size of the Alkyl Group, Int. J. Chem. Kinet., submitted, 2018.

Atkinson, R., Baulch, D. L., Cox, R. A., Crowley, J. N., Hampson, R. F., Hynes, R. G., Jenkin, M. E., Rossi, M. J., and Troe, J.: Evaluated Kinetic and Photochemical Data for Atmospheric Chemistry: Volume 1 – Gas Phase Reactions of O_x, HO_x, NO_x, and SO_x, Species, Atmos. Chem. Phys., 4, 1461-1738, 2004.

Atkinson, R., Baulch, D. L., Cox, R. A., Crowley, J. N., Hampson, R. F., Hynes, R. G., Jenkin, M. E., M. J. Rossi, and Troe, J.: Evaluated Kinetic and Photochemical Data for Atmospheric Chemistry: Volume II - Gas Phase Reactions of Organic Species, Atmos. Chem. Phys., 6, 3625-4055, 2006.

Carr, S. A., Baeza-Romero, M. T., Blitz, M. A., Pilling, M. J., Heard, D. E., and Seakins, P. W.: OH Yields from the $CH_3CO + O_2$ Reaction using an Internal Standard, Chem. Phys. Lett., 445, 108-112, 2007.

Dusanter, S., Vimal, D., and Stevens, P. S.: Technical note: Measuring tropospheric OH and HO_2 by laser-induced fluorescence at low pressure. A comparison of calibration techniques, Atmos. Chem. Phys. J1 - ACP, 8, 321-340, 2008.

Fuchs, H., Novelli, A., Rolletter, M., Hofzumahaus, A., Pfannerstill, E. Y., Kessel, S., Edtbauer, A., Williams, J., Michoud, V., Dusanter, S., Locoge, N., Zannoni, N., Gros, V., Truong, F., Sarda-Esteve, R., Cryer, D. R., Brumby, C. A., Whalley, L. K., Stone, D., Seakins, P. W., Heard, D. E., Schoemaecker, C., Blocquet, M., Coudert, S., Batut, S., Fittschen, C., Thames, A. B., Brune, W. H., Ernest, C., Harder, H., Muller, J. B. A., Elste, T., Kubistin, D., Andres, S., Bohn, B., Hohaus, T., Holland, F., Li, X., Rohrer, F., Kiendler-Scharr, A., Tillmann, R., Wegener, R., Yu, Z., Zou, Q., and Wahner, A.: Comparison of OH reactivity measurements in the atmospheric simulation chamber SAPHIR, Atmos. Meas. Tech., 10, 4023-4053, 10.5194/amt-10-4023-2017, 2017.

Hansen, R. F., Blocquet, M., Schoemaecker, C., Léonardis, T., Locoge, N., Fittschen, C., Hanoune, B., Stevens, P. S., Sinha, V., and Dusanter, S.: Intercomparison of the comparative reactivity method (CRM) and pump–probe technique for measuring total OH reactivity in an urban environment, Atmos. Meas. Tech., 8, 4243-4264, 10.5194/amt-8-4243-2015, 2015.

Parker, A., Amedro, D., Schoemaecker, C., and Fittschen, C.: OH Reactivity Measurments by FAGE, Environmental Engineering and Management Journal, 10, 107-114, 2011.